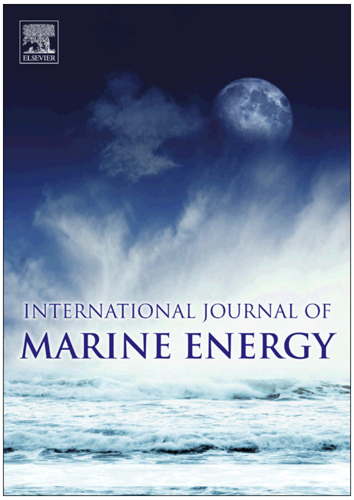

Visualising the aspect-dependent radar cross section of seabirds over a tidal energy test site using a commercial marine radar system

D.L. McCann, P.S. Bell

PII: S2214-1669(17)30002-4
DOI: http://dx.doi.org/10.1016/j.ijome.2017.01.002
Reference: IJOME 133

To appear in:

Received Date: 6 May 2015
Revised Date: 7 September 2016
Accepted Date: 11 January 2017

Please cite this article as: D.L. McCann, P.S. Bell, Visualising the aspect-dependent radar cross section of seabirds over a tidal energy test site using a commercial marine radar system, (2017), doi: http://dx.doi.org/10.1016/j.ijome.2017.01.002

Visualising the aspect-dependent radar cross section of seabirds over a tidal energy test site using a commercial marine radar system

D.L. McCann [a,*] & P.S. Bell [a]

[a] *National Oceanography Centre, Brownlow Street, Liverpool L3 5DA, UK*

[*] *Corresponding author. Tel.: +44 01517954810. E-mail address: dmca@noc.ac.uk (D.L. McCann).*

Abstract

The long-term monitoring of seabirds around proposed marine renewable energy (MRE) sites is vital to assess the large-scale and long-term environmental impacts of MRE installations. Marine radar could be a valuable tool to augment traditional seabird surveys but the problem of aspect dependency of the generic radar cross section (RCS) of live birds in flight must be understood before radar data is correctly interpreted. A marine radar multiple target tracking algorithm ('GANNET') was applied to data from an un-calibrated, horizontally polarised, 10kW X-band marine radar sited at the European Marine Energy Centre (EMEC) tidal renewable energy test site, Scotland U.K. From 24 days of data over 1.84 million target readings were recorded. For each target reading the radar aspect angle (bearing of radar beam incident on target), range and non-dimensional echo magnitude were derived allowing a view to be generated of the variation of echo magnitude with aspect angle for all tracked targets. The resulting polar diagram shows a significant change in echo magnitude with range between side-on and head/tail-on aspects indicating a large contribution of the RCS from the wings of birds in flight. The species-unspecific detectability of seabirds, especially at long range, is found to be strongly dependent on aspect angle. This has direct implications for the use of marine radar equipment for avian monitoring at proposed and active marine energy sites and must be taken into account if data from these radars are to be used to augment traditional bird abundance and area use surveys conducted by human observers.

Keywords:

Marine radar, Radar cross section, Environmental assessment, Marine ecology

Introduction

With increasing exploitation of coastal seas for marine renewable energy (MRE) there is a requirement to monitor changes in the marine ecosystem directly or indirectly affected by the MRE industry . As such, there is an increased need for ecological monitoring systems that can work over large areas and long time periods, potentially continuously, in order to better characterise changes in the marine ecosystem; especially if the MRE sector is to move away from overly-conservative assumptions for Environmental Impact Assessments (EIAs), a vital part of the consenting and approval process for MRE projects. Current monitoring strategies involving shore- or vessel-based human observers are applied to attempt to produce maps of spatial overlap but are limited (currently) to daytime operation and the duration of observer presence. Additional problems with observer-based, visual surveys over wide areas suited to marine energy development (seabirds present on the sea surface) were found by , with viable analyses requiring sacrifices in the form and quality of data used.

Radar (an acronym of radio detection and ranging), in its many forms, has been a valuable tool for avian research since the identification of the radar echoes dubbed ‘angels’ by British pilots in WWII as those generated by birds in flight , , being found operating both on local and national scales and especially around aerodromes. Radar has also been used extensively to monitor seabirds around offshore wind turbine installations to varying degrees of success . Although a powerful tool for avian research, radar data has certain limitations and caveats that must be thoroughly understood before interpretation of the data .

The National Oceanography Centre (NOC) has been operating a marine X-band radar station as part of the Flow and Benthic Ecology 4D (FLOWBEC 4D) project overlooking the waters of the European Marine Energy Centre (EMEC) on the Island of Eday, North Scotland U.K. The tidal race offshore of Eday (‘the Fall of Warness’, FOW) is home to numerous tidal stream turbine research and demonstration projects and as such is a prime candidate for the testing of long-term monitoring strategies which should be deployed alongside the numerous tidal stream MRE developments planned for the future in European waters. Part of the NOC operational radar oceanography suite comprises a research-grade multiple small target tracking program 'GANNET', capable of detecting and tracking small targets on or above the sea surface. As the NOC radar is non-coherent and un-calibrated GANNET has been extensively tested and tuned to maximise the number of target detections while simultaneously minimising false alarms due to other high-magnitude scatterers such as sea spikes and precipitation. The result is a set of algorithms that is consistently capable of identifying and tracking the radar echoes from birds in flight while minimising the effect of backscatter due to sea clutter (**Fig. 1**). Although not presently validated through visual observations the echoes due to seabirds are identifiable due to their apparent motion in successive radar images ; being high-velocity, high magnitude (compared with the low sea state clutter) and displaying the kinematic behaviour of seabirds in flight over coastal waters. This *a priori* information is the basis of the following analysis; the majority of automatic bird tracking algorithms require human input at some point in the process and here it exists as the end result of model tuning.

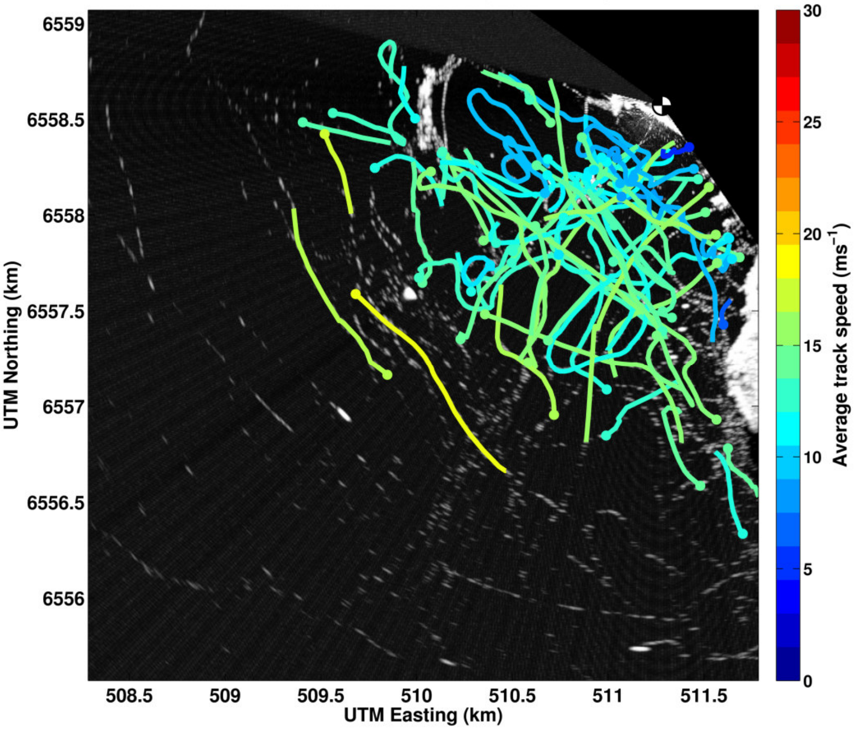

Fig. 1. Example output from GANNET from 256 frames of radar data (5.5 minutes) showing bird tracks coloured by average track speed (ms^{-1})

A persistent problem associated with radar-based automatic detection and tracking algorithms is the unknown effect of the target's material composition and orientation relative to the beam on the scattering of microwave energy back to the antenna. This is manifest as the target radar cross-section σ in the radar equation

$$P_r = \frac{P_t G_t A_r \sigma}{(4\pi R^2)^2}$$

where P_r is the received (back-scattered) power, P_t is the transmitted power, G_t is the transmitted gain (a function of beam shape), A_r is the receiver antenna effective area and R is the range to target. In order to make a quantitative assessment of σ it is a requirement that P_r, P_t and R be measured (the other parameters may be estimated or taken from the radar antenna's technical documentation). This process is known as radar calibration and involves the sounding of a target with a known σ (e.g. a steel sphere with a 1m^2 aspect area) at various ranges. This calibration is time consuming and rarely, if ever, conducted for a commercial marine radar system. Radars powered by magnetron transmitters also present the problem of a fluctuating power output over time, rendering the calibration valid only for a short period.

A major issue arising from the dependency of σ on the radar-target aspect angle (angle between the incident radar beam and the target's major axis) is that there exists the possibility that automatic detection and tracking systems (e.g. GANNET) may be effectively blind to targets at particular aspect angles. If a system such as GANNET is to be used operationally to enumerate and characterise bird activity over MRE sites, augmenting and extending the work of , there must be a prior exploration of this dependency and its impact on the tracking results. Is the system characterising an area as being free of birds because there are none there or because it cannot see them? This is also a known problem with human observer surveys where poor visibility due to weather and sea state, light levels or the narrow field of view a human observer can obtain with optical instruments many birds go unobserved even when they are present.

Although the aspect-dependency of the RCS of birds is a well-known phenomenon in the field of radar ornithology there is a paucity of accessible literature (and written in English) that have published empirical results of avian RCS experiments. Of the literature available a small selection deals with commercially available X-band radars increasingly used to monitor MRE sites. Early work by displayed an aspect angle dependency of the radar echo from a variety of birds using a horizontally-polarised X-band radar but they were neither alive (being deceased birds suspended on a thread), nor in active flight during measurements. The study also attempted to show that the feathers of a bird are largely transparent in X-band by plucking a bird and illuminating a polythene bag stuffed full of its feathers, however the lack of liquid blood in the dead feathers (live feathers are partially vascularised) will have greatly reduced their reflectivity in X-band. Later work by on the radar cross section of live ducks and chickens was commendable for the author's dedication to the training of the animals to remain still while illuminated by a microwave radar beam on a rotating pedestal but the conclusions are suspect due to the lack of experimental description and the low frequency of the radar used (400MHz, or ~17cm). While the authors did not succeed in solving the RCS problem for live birds they did conclude with a very good recipe book for duck. In both cases the author's conclusions that a bird's wing area makes no significant contribution to the radar cross section is dubious due to the problems with experimental method – in neither case was a bird illuminated while in flight. argues that the previous research failed to account for the potential Bragg-resonant response of the wings of many species of birds that tend to have dimensions that are modes of commonly used X-band wavelengths and it is the changing wing geometry in flight that may be responsible for the observed backscatter modulation at the wing-beat frequency which has been subsequently observed(, ,). calculated the aspect-dependent radar cross section of a selection of small birds and Geese flocks over an aerodrome in X-band but were only able to due to measurements of an Airbus A320 aircraft that passed through the beam and the known RCS of that aircraft model was used to calibrate data from the birds. An aspect-dependent RCS diagram of a gull (no species given) is presented in , however no explanation is given to the nature of the measurements or indeed the radar used.

Although it is impossible to calculate a true RCS for a target with an un-calibrated radar system there remain extensive possibilities to characterise its effects on the non-dimensional echo magnitude recorded in digitised radar images such as are used by GANNET. Many radar-based avian monitoring radars use parabolic antennas with pencil-beams (e.g., ,) providing good ground (or sea) clutter suppression and a target elevation determination. The use of commercial, marine surveillance X-band equipment (i.e., slotted waveguide antennas with fan-shaped beams, magnetron-amplified transmitters) for avian surveying is limited but its presence in the marine sector is ubiquitous, being mounted on the majority of vessels at sea. There are a limited number of commercial bird-tracking X-band radars that utilise slotted waveguides (e.g., the Robin Radar system used in), however detailed information on their workings is not openly available. The present work was conducted, in part, to augment the current NOC radar oceanography toolbox with a bird tracking capability, using only digitised radar images, commercially available hardware and limited *a priori* target information.

Birds at the FOW site

Shore-based bird survey work carried out on behalf of EMEC (,) and later shore- and boat-based survey work conducted as part of the FLOWBEC project found the majority of sea birds at the FOW to be common guillemots *Uria aalge*, black guillemots *Cephus grille*, eider ducks *Somateria mollissima*, European shags *Phalacrocorax aristotelis*, Arctic terns *Sterna paradisaea*, kittiwakes *Rissa tridactyla*, Northern gannets *Morus bassanus*, Atlantic puffins *Fratercula arctica*, great cormorants *Phalacrocorax carbo* and razorbills *Alca torda*. This non-exhaustive list of species present at the FOW presents a range of target types to the radar. Reported flight speeds of these species range from ~10ms-1 for terns to over 19ms-1 for eider ducks and a large range of body masses and wing spans are present . Additionally the range in flight and foraging behaviours (flight altitude / sea surface behaviour / circling etc.) present a large range of target types for GANNET to track. While some speciation of identified targets may be possible using flight speed or track behaviour this was not conducted for the present study.

Material and methods

The NOC small target tracking algorithm GANNET is a simple, yet robust, implementation of the Global Nearest Neighbour tracking program of with modifications for use with digitised X-band radar images. The program is comprised of five sections:

1) Target detection via thresholding
2) Target identification via Connected Component Labelling (CCL) analysis
3) Clutter suppression using Clutter-Map Constant False Alarm Rate (CM-CFAR)
4) Target-to-track data association through the solution of the Munkres algorithm
5) Track state update via an Extended Kalman Filter (EKF).

Target detection is achieved at the pixel level using a simple thresholding procedure between an individual image pixel I_p, the mean pixel value over 256 frames $\overline{I_p}$ and two tuneable parameters a and b so that a target is detected if

$$I_p > (\overline{I_p}a + b) \qquad 1$$

is satisfied.

Due to the footprint of the radar beam a target may be illuminated in multiple azimuth and range bins creating a 'blob' in the resulting Cartesian transformed radar image. In order to track each target these ‘blobs’ must be converted to point targets ,achieved through target identification and pixel association via CCL (based on methods found in). Here each target pixel cluster is assigned an integer number within a single scan and the centre of mass calculated in geographic Cartesian coordinates (UTM projection). Any targets consisting of a single, unconnected pixel are rejected at this stage and attributed to noise or clutter. Each target is stored in state-space with 4 degrees of freedom (*x* and *y* coordinates, target magnitude and cluster size).

The CM-CFAR routine is a simple method based on the number of identified targets (plus false alarms) found in a finite area of the image to produce a binary 'clutter-map'. When the number of identified targets reaches a tuneable threshold the analysis removes that area of the image (and any identified targets therein) from any subsequent tracking. This is a simple, yet heavy-handed filtering method that has the effect of removing all but very light sea clutter from the analysis. Unfortunately this also reduces the effective operation of GANNET to tracking targets over low sea states (WMO sea state < 2) . **Fig. 2** shows the effect of the adopted CM-CFAR routine on images with low (left) and medium (right) clutter environments. The images were created by storing the maximum echo intensity of each azimuth/range pixel over a 256 scan (~5 minute) period which is a convenient way to visualise areas of ground/sea clutter and the tracks of birds. Bird tracks appear as a line of dots representing the position of the target during each antenna rotation.

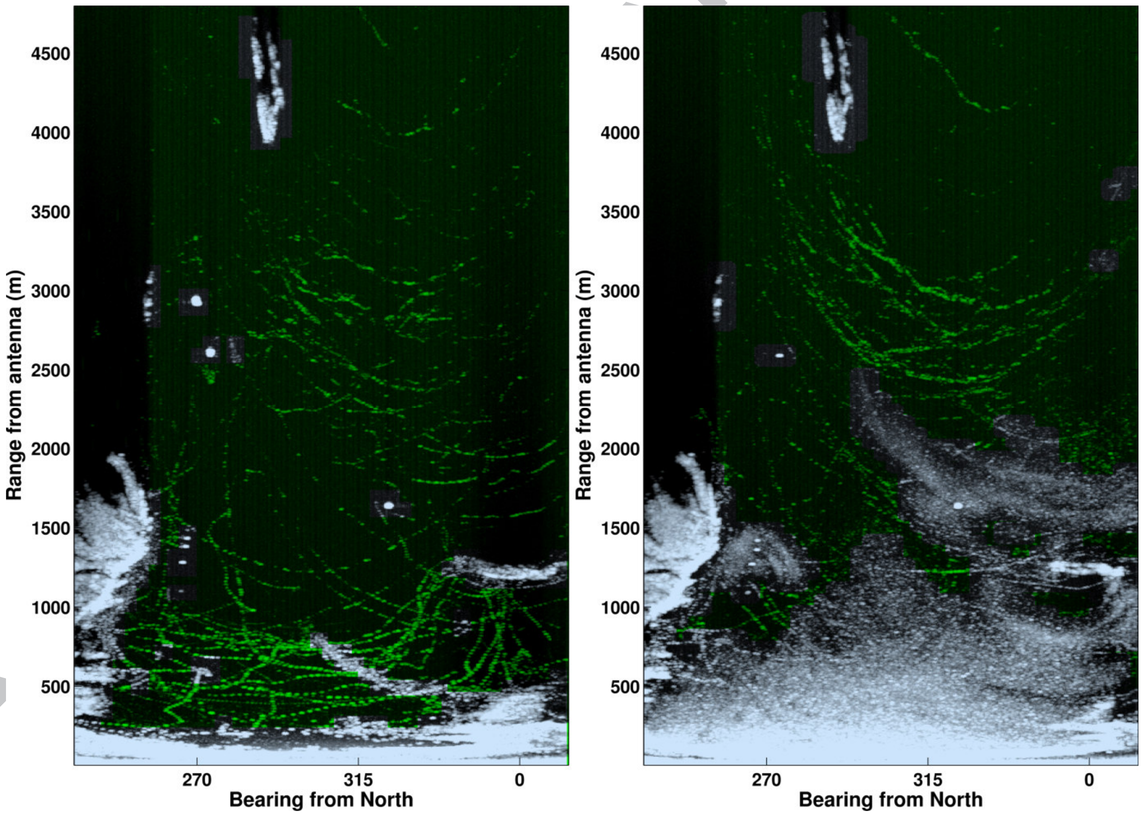

Fig. 2. Maximum echo intensity images for low (left) and medium (right) clutter cases. Areas of the images removed from the analysis by the CM-CFAR routine are coloured white while areas remaining for tracking are coloured green.

Data association is achieved through solution of the Munkres assignment algorithm and the gating routine proposed by . Once associations have been made, house-keeping is undertaken (track initiation and removal) and track state update is performed using an Extended Kalman Filter (EKF). The measurement and process noise covariance matrices of the EKF were tuned manually; with the process noise covariance matrix estimated using the method of . The target dynamic model within the EKF was chosen to be a Singer acceleration model . Track house-keeping only included the removal and initiation of tracks and therefore no connecting of tracks that may belong to the same target. Without a more sophisticated multiple target tracking algorithm or further target information (e.g. Doppler speeds, measured RCS using a calibrated radar etc.) the association of targets between tracks is not possible. This could have the effect of over-estimating the number of targets in an area as targets can be effectively counted multiple times per scan set and across sampling periods if the target remains in the radar field of view.

The radar system used in this survey was a Kelvin Hughes X-band unit (9.4GHz / 3.8cm) coupled to a 2.4m horizontally polarised slotted waveguide (‘T-bar’) antenna rotating at approximately 46rpm. The transmit power was set to 10kW with a pulse length of 50ns. The antenna is mounted on a pole approximately 7m above mean sea level and produces a fan-shaped beam with a horizontal 3dB beam width of 0.8° and a vertical beam width of ±20° from the horizontal. The raw radar video signal was intercepted and sampled by an OceanWaves GmbH WaMoS II radar digitiser working at 30MHz to produce digitised images every antenna scan with an azimuthal angular resolution of 1/3° and a radial range resolution of 4.7m to a maximum range of 4km. These images were then stored to hard disk every 256 scans with a recording/storage cycle every 11 minutes.

Theory / calculation

GANNET was run on radar images recorded concurrent with two of the FLOWBEC sea-bed frame deployments in the FOW (14th–26th June 2012 and 3rd–15th June 2013, described in). In total, 3094 survey records were processed containing 256 radar images each. Across the combined data set

GANNET identified a total of 80,000 tracks comprised of over 1.84 million individual target readings (an average of 23 target measurements per track), however as stated previously the number of tracks does not directly relate to the number of individual targets present in the area due to the problem of track-to-track association both within and across recording periods. The CM-CFAR routine rejected an average of 22.5% of the radar images over the dataset with a maximum of 71.1% (an example with heavy sea and rain clutter) and a minimum of 10.8% (due to ground clutter). The track direction for each target observation was derived from the recorded track files to determine the target bearing angle *a* (**Fig. 3**. For each observation where the target bearing could be determined it was combined with the radar pulse azimuth *b* to resolve the target aspect angle *c*.

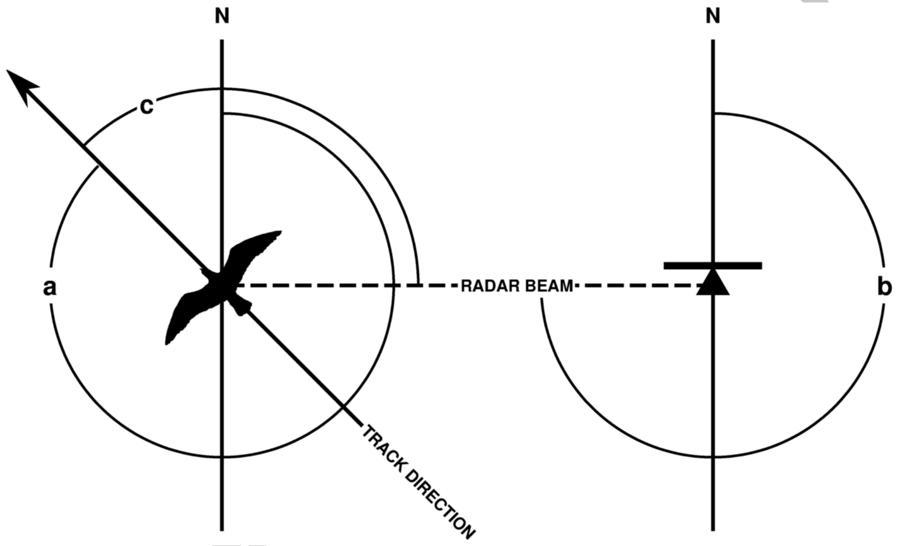

Fig.3. Angles present in the detection problem: the target bearing from North (*a*), the radar pulse azimuth measured from North (*b*) and the target aspect angle (*c*).

The local wind speed and direction was not taken into account when calculating the target track direction as no detailed, fine-scale directional wind information was available for the area studied. Wind has the potential to affect the angle between the bird's orientation and flight track direction if the specimen is flying with the wind taken into account to reach a certain destination (much as an aeroplane pilot does). For a small number of measured targets this could present a problem for the calculation of aspect-dependent echo response, however for the number of targets identified and measured in this study it is assumed this wind effect will not impact the results.

As the radar was un-calibrated there is no formal way of determining the RCS of any of the targets identified and tracked by GANNET. However, information on their relative echo magnitude, cluster size and target aspect angle was available for the 1.84 million target readings. Combined with the assumption that the majority of targets that survive the CM-CFAR screening process are seabirds and that the majority of GANNET output images (e.g. **Fig. 1**) display either realistic flight tracks and speeds or none at all, the information on target flight track direction (and therefore radar aspect angle) may be used to demonstrate the aspect-dependent variation of the echo magnitude of seabirds in flight.

The final result is not valid for any particular species of seabird, but for seabirds in general. There is additional complication in that although GANNET is capable of distinguishing between individual targets in a group the nature of the input imagery sometimes causes multiple targets to be treated as one. However, the aspect-dependent RCS with relation to the contribution of wing geometry in flight should be broadly shared amongst all seabirds as they all share similar body shapes (generally fusiform body, size of the order cm to m) and they all utilise wings to fly. As the radar samples a volume above the sea surface GANNET is also unable to distinguish the flight altitude of any target it tracks. Due to the fan shape of the radar beam (0.8° and 20° horizontal and vertical beam-widths) this volume is expected to extend to approximately 200m above sea level at 1km range, expanding to approximately 680m at 4km range.

Results

For the 1.84 million aggregated target measurements from GANNET the radar aspect angle, non-dimensional echo magnitude and range from antenna were stored. The echo magnitude is represented by a digitised 12-bit integer number and its derivation is performed within the WaMoS II analogue to digital converter. The aspect angles and echo magnitudes were then binned into range-aspect angle space with resolutions of 1° in aspect angle and 10m in range so that each bin contains the sum of all echo magnitudes across all target pixels within that bin, divided by the number of targets present.

Fig. 4. shows an image of the binned echo magnitudes (normalised with the overall maximum) for the aspect-angle / range bins. The WaMoS II analogue-to-digital converter performs a degree of range-dependent scaling to the resulting echo magnitude that is poorly documented, although this is unlikely to affect the aspect-dependency of the signal present in **Fig. 4**.Included on the plot is a black line representing the aspect angle averaged echo magnitude with the values normalised to fit within the 4km range ring of the plot.. Firstly, two distinct lobes can be seen in the data around the 90° and 270° bearing marks. These two directions represent the side-on aspect of the collated targets. These lobes are further represented by the average echo line which reaches its maximum around these two aspect angles. There are two likely explanations for this. Firstly, the generally fusiform body shape of all seabirds presents a larger physical target area to the antenna broadside than head-on. This is a known result as observed by . Secondly the wings, as they flap between two points in a cycle either create a larger target area geometrically (when extended fully up or down) or reach a point in the cycle that possibly instigates a Bragg-resonant response and greatly increases the echo magnitude. The internal composition of a bird's wing is, from a radar's point of view, identical to that of the body, being formed of predominantly fluids (e.g. water and blood) that are highly radar reflective .

Two minima can be observed within the lobes at the 90° and 270° marks just above the 1.5km range ring, corresponding to the position of the intertidal skerries 1.5km West of the radar installation. As GANNET is less likely to detect targets over the high-amplitude returns from the rocky outcrop this results in a corresponding decrease in the probability of detection and the collated echo magnitudes recorded over that area.

Much of **Fig. 4** around the 0° and 180° aspect angles display comparatively low echo magnitudes or no data at all. These minima are at the core of the detection problem: Are there no seabirds flying towards or away from the beam at ranges greater than 1km or are they relatively invisible to the radar? Over 1.84 million measurements and over a total time period of a month it is statistically unlikely that the former is true.

The effectiveness of the CM-CFAR filter will have a small effect on **Fig.4.** through the addition of false alarms in the tracking process. However the addition of sea clutter, if GANNET tracks sea spikes in the direction of wave travel, should produce the opposite RCS signal as the Bragg-resonant response of waves tends to zero for waves travelling across the radar beam (i.e. looking along wave crests) .

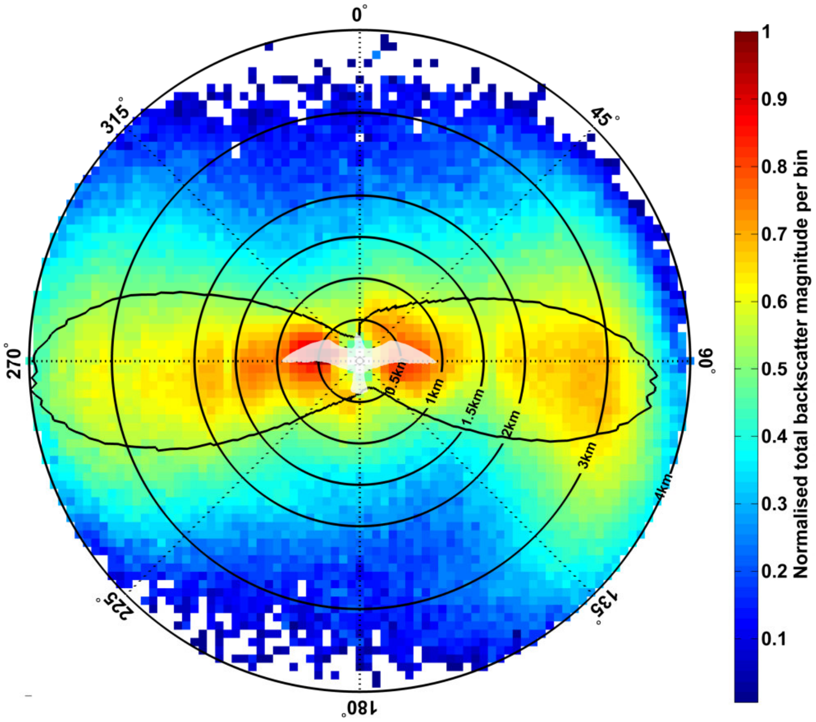

Fig. 4. The normalised total echo magnitude for each aspect angle-range bin with aspect angles and range rings (from the antenna) plotted for reference. The black line overlain represents the average normalised total echo magnitude for each aspect bearing, normalised to the 4km range ring. A seabird silhouette is added for reference.

Discussion and conclusions

The measurement of true RCS, defined by the radar equation, is impossible without a calibrated radar system and even if it was it would only be valid for a particular radar frequency. The RCS would also only be formally valid for a single species and a certain body size (and therefore age due to an individual's growth). This is one of the major issues with using target RCS for identification purposes; it is possible when the target is well defined and universal (e.g. a model of aircraft) but may not be particularly useful for biological organisms that display vast divergences in shape, size and behaviour.

Visual representations of the aspect-dependent echo response of flying seabirds are rare in the available literature; with the few examples that do exist being either limited to immobile or deceased specimens (,) or do not include any or enough explanatory information to accompany the RCS diagram (,). An even larger portion of referenced literature on the subject is not readily available (e.g. the Royal Radar Establishment memorandums referenced in ; unavailable even through the National Archives). This work therefore serves to provide available information on the detectability of flying seabirds with marine radar; as large-scale, automated bird surveys become more important over marine renewable energy installations there must be an in-depth understanding of what information the radar provides. Radar-based avian monitoring is a valuable tool to compliment traditional visual surveying; especially in situations where human observers are not as capable (e.g., at night or in high target density environments). The combination of long range, 24-hour surveying and multiple-target tracking capability can provide MRE sites a hugely valuable data resource to contribute to the EIA and consenting process as well as continuous monitoring.

This work shows that using simple commercial radar and digitiser hardware, a relatively simple set of tracking algorithms, a large data set and a degree of *apriori* information it is possible to visualise the aspect-dependent RCS of seabirds in flight in their natural environment. The implications of the results presented for the automatic monitoring of seabirds over MRE sites are twofold: Firstly, simple marine radar equipment is capable of detecting and tracking birds over low-clutter conditions over wide areas and long periods, thus providing a valuable tool for the removal of overly-conservative assumptions in EIAs as part of the consenting and approval process for MRE sites. Secondly, the aspect-dependent RCS must be taken into account when using a traditional marine radar (i.e., with a horizontally scanning slotted waveguide antenna) as the detection probability of flying birds is considerably lower at certain aspect angles; with the potential to miss the detection of a target in certain circumstances and geometries.

Although there is no way to account for target altitude with a scanning antenna of the type used in this study there is potential to distinguish between flying and floating seabirds using kinematic behaviour recorded by a tracking algorithm such as GANNET combined with surface current information; potentially from a tidal model or measured using the same radar system . Further work is required to quantify this result in terms of the species-level differences between seabirds. An ideal solution would be to analyse data from two, simultaneous radars illuminating targets with aspect angles differing by 90°, however practical and cost restraints may preclude this for future projects.

Acknowledgements

The small target tracking methodology was funded by the NERC Marine Renewable Energy Knowledge Exchange Programme on the basis of a broader industry need acknowledged by the European Marine Energy Centre (EMEC) and the companies participating in EMEC Developer Research Forum (see http://www.emec.org.uk/emec-developer-research-forum/). Further development and data gathering was supported by the NERC & DEFRA funded project FLOWBEC, under grant number NE/J004332/1, and additional support from the National Oceanography Centre, UK.

We would also like to thank Dr. James Waggitt for helpful discussions on the shaping the outputs of the algorithms for application to studies of sea bird behaviour.

References

[1] R. Langton, I. Davies and B. Scott, “Seabird conservation and tidal stream and wave power generation: Information for predicting and managing potential impacts.,” *Marine Policy,* vol. 35, p. 623–630, 2011.

[2] J. Waggitt and B. Scott, “Using spatial overlap to estimate the risk of collisions between deep diving seabirds and tidal stream turbines: A review of potential methods and approaches.,” *Marine Policy,* vol. 44, p. 90–97, 2014.

[3] J. Waggitt, P. Bell and B. Scott, “An evaluation of the use of shore-based surveys for estimating spatial overlap between deep-diving seabirds and tidal stream turbines,” *International Journal of Marine Energy,* vol. 8, p. 36–49, 2014.

[4] I. Buss, “Bird detection by radar,” *The Auk,* vol. 63, p. 315–318, 1946.

[5] W. Harper, “'Angels' on centimetric radars caused by birds,” *Nature,* vol. 180, p. 847–849, 1957.

[6] S. Gauthreaux Jr. and C. Belser, “Radar ornithology and biological conservation,” *The Auk,* vol. 120, p. 266–277, 2003.

[7] T. Nohara, R. Beason and P. Weber, “Using radar cross-section to enhance situational awareness tools for airport avian radars,” *Human-wildlife Interactions,* vol. 5, p. 210–217, 2011.

[8] M. Desholm, A. Fox, P. Beasley and J. Kahlert, “Remote techniques for counting and estimating the number of bird-wind turbine collisions at sea: A review,” *Ibis,* vol. 148, p. 76–89, 2006.

[9] R. Beason, T. Nohara and P. Weber, “Beware the Boojum: caveats and strengths of avian radar,” *Human-wildlife Interactions,* vol. 7, p. 16–46, 2013.

[10] P. Bell, D. McCann, B. Scott, B. Williamson, J. Waggitt, I. Ashton, L. Johanning, P. Blondel, A. Creech, D. Ingram, J. Norris, M. Finn, R. Torres, P. Cazenave, D. Conley, D. Greaves, Savidge G., E. Armstrong, C. Hall, R. Kennedy and J. O'Carroll, “FLow and Benthic ECology 4D - FLOWBEC - an overview,” in *Proceedings of the 2nd International Conference on Environmental Interactions of Marine Renewable Energy Technologies (EIMR2014)*, Stornoway, Ilse of Lewis, Scotland U.K., 28th April – 2nd May 2014.

[11] P. Stepanian, P. Chilson and J. Kelly, “An introduction to radar image processing in ecology,” *Methods in Ecology and Evolution,* vol. 5, p. 730–738, 2014.

[12] R. Skolnik, Radar Handbook, New York, U.S.A.: McGraw-Hill, 1970.

[13] H. Schmaljohann, F. Leichti, E. Bächler, T. Steuri and B. Bruderer, “Quantification of bird detection by radar - a detection probability problem,” *Ibis,* vol. 150, p. 342–355, 2008.

[14] J. Edwards and E. Houghton, “Radar echoing polar diagram of birds,” *Nature,* vol. 184, p. 1059, 1959.

[15] P. Blacksmith and R. Mack, “On measuring the radar cross section of ducks and chickens,” *Proceedings of the IEEE,* vol. 53, p. 1125, 1965.

[16] C. Vaughn, “Birds and insects as radar targets: A reniew,” *Proceedings of the IEEE,* vol. 73, p. 205–227, 1965.

[17] S. Zaugg, G. Saporta, E. Van Loon, H. Schmaljohann and F. Leichti, “Automatic identification of bird targets with radar via patterns produced by wing flapping,” *Journal of the Royal Society Interface,* vol. 5, p. 1041–1053, 2008.

[18] F. Leichti and L. Bruderer, “Wingbeat frequency of barn swallows and house martins: a comparison between free flight and wind tunnel experiments,” *Journal of Experimental Biology,* vol. 205, p. 2461–2467, 2002.

[19] A. Dokter, M. Baptist, B. Ens, K. Krijgsveld and E. van Loon, “Bird radar validation in the field by time-referencing line-transect surveys,” *PLoS ONE,* vol. 8, p. doi:10.1371/journal.pone.0074129, 2013.

[20] DMP Statistical Solutions UK Ltd., “Analysis of bird data for the Fall of Warness area: A report prepared for AURORA Environmental Limited.,” 2006.

[21] SMRU Ltd, “Analysis of bird data for the Fall of Warness area, Orkney: Final report for EMEC,” 2007.

[22] C. Pennycuick, “Actual and 'optimum' flight speeds: Field data reassessed,” *Journal of Experimental Biology,* vol. 200, p. 2355–2361, 1997.

[23] J. Kahlert, I. Petersen, A. Fox, M. Desholm and I. Clausager, “Investigations of birds during construction and operation of Nysted offshore wind farm at Rødsand,” 2003.

[24] P. Konstantinova, A. Udvarev and T. Semerdjiev, “A study of a target tracking algorithm using global nearest neighbor approach,” in *Proceedings of the International Conference on Computer Systems and Technologies (CompSysTech)*, Sofia, Bulgaria, 19th–20th June 2003.

[25] M. Haralick and L. Shapiro, Computer and robot vision, Boston: Addison-Wesley Publications, 1992.

[26] J. Munkres, “Algorithms for the assignment and transportation problems,” *Journal of the Society for Industrial and Applied Mathematics,* vol. 5, p. 32–38, 1957.

[27] S. Särkkä, “On unscented Kalman filtering for state estimation of continuous-time nonlinear systems,” *IEEE Transactions on Automatic Control,* vol. 52, p. 1631–1641, 2007.

[28] R. Singer, “Estimating optimal tracking filter performance for manned manoeuvring targets,” *IEEE Transactions on Aerospace and Electronic Systems,* Vols. AES-6, p. 473–483, 1970.

[29] B. Williamson, P. Blondel, E. Armstrong, P. Bell, C. Hall, J. Waggitt and B. Scott, “A self-contained subsea platform for acoustic monitoring of the environment around marine renewable energy devices—Field deployments at wave and tidal energy sites in Orkney, Scotland,” *IEEE Journal of Oceanic Engineering,* vol. 41, p. 67–81, 2015.

[30] J. Wright, “Backscattering from capillary waves with application to sea clutter,” *IEEE Transactions on Antennas and Propagation,* vol. 14, p. 749–754, 1966.

[31] K. Hessner, K. Reichert, J. Borge, C. Stevens and M. Smith, “High-resolution X-Band radar measurements of currents, bathymetry and sea state in highly inhomogeneous coastal areas,” *Ocean Dynamics,* vol. 64, p. 989–998, 2014.

Highlights

- Data from a shore-based, marine X-band radar is used to detect and track flying seabirds over the waters of the European Centre for Marine Energy (Scotland, U.K.)
- The radar cross section of flying seabird targets is visualised using the output of a multiple target tracking algorithm
- The radar cross section of flying seabirds is found to be highly aspect dependent, with significantly larger contributions from the wings
- The results of the study have impacts for future X-band radar based seabird monitoring activities over proposed marine renewable energy sites